Analysis of experimentally validated trans-ionospheric attenuation estimates of VLF signals

K. L. Graf,[1] N. G. Lehtinen,[1] M. Spasojevic,[1] M. B. Cohen,[1] R. A. Marshall,[1] and U. S. Inan[1,2]

Received 7 February 2013; revised 6 March 2013; accepted 12 March 2013.

[1] Accurate models of trans-ionospheric propagation are needed to assess the role of Earth-originating very low frequency (VLF) electromagnetic waves in radiation belt dynamics. Recent studies have called the relatively crude early trans-ionospheric models into question, finding that they underestimate the attenuation by 20–100 dB. A full wave model that includes all of the relevant physics has recently become available and experimentally verified to within a few decibels via comparison to more extensive satellite data. Using this model, we discuss the importance of wave polarization, incidence angle, bearing, ground conductivity, horizontal distance from the source, and the ionospheric profile, all of which are demonstrated to play a significant role in the trans-ionospheric propagation. Trans-ionospheric attenuation estimates are provided both for the case of vertical incidence of a whistler-mode wave and for the case of magnetospheric injection from a dipolar terrestrial VLF source. These estimates agree with observation to within ±6 dB. The remaining discrepancy may be attributable to ionospheric variation and/or factors not captured by our horizontally stratified model. On the basis of the full wave treatment presented herein, we find that the earlier work showing a >20 dB overestimation by traditional models results from the unrealistic simplifying assumption that the wave is vertically incident onto the ionosphere, exacerbated by the fact that most of the satellite data used for comparison came at large horizontal distances (hundreds of kilometers) from the source.

Citation: Graf, K. L., N. G. Lehtinen, M. Spasojevic, M. B. Cohen, R. A. Marshall, and U. S. Inan (2013), Analysis of experimentally validated trans-ionospheric attenuation estimates of VLF signals, *J. Geophys. Res. Space Physics*, *118*, doi:10.1002/jgra.50228.

1. Introduction

[2] Very low frequency (VLF) electromagnetic waves play an important role in controlling the evolution of energetic electron distributions in near-Earth space. When propagating in the magnetosphere in the whistler mode, VLF waves can induce pitch-angle scattering and precipitation of trapped energetic particles [e.g., *Imhof et al*., 1983; *Inan*, 1987]. *Abel and Thorne* [1998a] studied the dominant factors in such electron scattering losses in the inner magnetosphere and concluded that VLF waves radiated from lightning discharges, and terrestrial anthropogenic transmitters play a significant role in maintaining the slot region of depleted fluxes between the inner and outer radiation belts. A critical factor in such a study, however, is quantifying the amount of VLF energy which penetrates from a terrestrial source, through the ionosphere, and into the magnetosphere.

[3] Magnetospherically generated VLF emissions such as chorus and hiss are also extremely important in radiation belt dynamics, and in the absence of local measurements, ground-based recordings of these waves can be used to estimate characteristics of the in situ distribution [*Horne et al*., 2005; *Spasojevic and Inan*, 2005; *Golden et al*., 2011]. However, using ground-based data to quantitatively estimate in situ wave power [e.g., *Golden et al*., 2010] requires knowledge of how efficiently the VLF waves penetrate downward from the magnetosphere through the ionosphere and into the Earth-ionosphere waveguide. Similarly, understanding trans-ionospheric propagation is an important aspect of using ground-based or space-based whistler measurements to remotely sense plasmaspheric electron densities [e.g., *Carpenter*, 1966; *Carpenter et al*., 1981; *Lichtenberger et al*., 2008; *Lichtenberger*, 2009].

[4] Despite the fact that quantitative estimates of trans-ionospheric attenuation of VLF waves are important for many studies in space sciences, the preeminent reference for many of these studies [e.g., *Abel and Thorne*, 1998a; *Bortnik et al*., 2002; *Kulkarni et al*., 2008; *Starks et al*., 2008; *Golden et al*., 2010] has been Figure 3-35 of

[1]Department of Electrical Engineering, Stanford University, Stanford, California, USA.
[2]Electrical Engineering Department, Koc University, Istanbul, Turkey.

Corresponding author: K. L. Graf, Department of Electrical Engineering, Stanford University, 350 Serra Mall, Room 308, Stanford, CA 94305, USA. (graf@stanford.edu)

2169-9380/13/10.1002/jgra.50228

Helliwell [1965]. The trans-ionospheric absorption estimates of *Helliwell* [1965] were presented at the time with several known caveats, and recent in situ satellite observations [e.g., *Starks et al*., 2008] have further questioned their validity. Helliwell presented the total trans-ionospheric absorption of an electromagnetic whistler-mode wave through the ionosphere as a function of geomagnetic latitude for representative frequency and day/night conditions. Helliwell made simplifying approximations to facilitate the numerical computation of these curves, and they were originally intended only for midlatitude and high-latitude analysis of whistler-mode waves incident upon the ionosphere with their wave normals within the cone of transmission [*Helliwell*, 1965, section 3.7]. *Inan et al.* [1984] combined the waveguide power model developed by *Crary* [1961] with Helliwell's trans-ionospheric absorption curves to estimate transmitter power above the ionosphere. *Starks et al.* [2008] combined this approach with the Air Force Research Laboratory's VLF Propagation Code to produce a three-dimensional model for illumination of the plasmasphere by terrestrial VLF transmitters. In comparing their model to measurements from dozens of satellite passes over several VLF transmitters, *Starks et al.* [2008] concluded that *Helliwell* [1965] underestimates the 20 kHz midlatitude attenuation by about 10 dB in the day and 20 dB during the night. *Tao et al.* [2010], applying a full wave method for trans-ionospheric absorption but again looking at single incident plane waves with vertical incidence, analyzed *D* region electron density variation and suggested that even more discrepancy (up to 100 dB) may be present when using more realistic electron density profiles.

[5] A series of studies attribute all or portions of this discrepancy to nonlinear effects and/or scattering from irregularities [e.g., *Foust et al*., 2010; *Bell et al*., 2011; *Shao et al*., 2012]. Theoretical calculations of *Foust et al.* [2010] attribute up to 3–6 dB of loss to scattering of whistler-mode waves from magnetic field-aligned density irregularities in the *F* region. *Shao et al.* [2012] attribute up to 9–15 dB of loss to conversion to lower hybrid waves in the *D* and *E* regions. The "smooth ionosphere" models of *Helliwell* [1965], *Lehtinen and Inan* [2009], and *Tao et al.* [2010] do not account for these effects, and it is unknown how much and how often nonlinear and scattering phenomena affect the trans-ionospheric propagation of VLF waves.

[6] Recent findings by *Cohen and Inan* [2012] and *Cohen et al.* [2012] provide the first cases of consistent agreement between satellite-based observations and modeling results for magnetospheric injection from terrestrial VLF transmitters. *Cohen and Inan* [2012] analyzed thousands of DEMETER satellite passes over 6.5 years over each of a dozen VLF transmitters to provide radiation maps at 700 km altitude with 25 km resolution, providing significantly more averaging and spatial resolution than previous studies on this topic. Using these maps, the total power injected into the magnetosphere from each transmitter was calculated for both daytime and nighttime. *Cohen et al.* [2012] compared these power estimates to those of a full wave method (FWM) model described by *Lehtinen and Inan* [2008, 2009], finding that the model correctly reproduces the injected VLF power to within ± 6 dB for both daytime and nighttime for each and every one of the 12 transmitters considered. It should be noted that the full wave model is a "smooth ionosphere" model that does not include ionospheric density irregularities, indicating that those irregularities may play a much smaller role than has been proposed. For instance, the model-data agreement was shown not to be a function of transmitter power up to 1 MW, which does not support the suggestion by *Shao et al.* [2012] that transmitter-induced irregularities such as those observed by *Parrot et al*. [2007] and *Bell et al.* [2008] play a significant role in trans-ionospheric absorption.

[7] Given the findings of *Cohen and Inan* [2012] and *Cohen et al.* [2012], in this paper we use the FWM to compute trans-ionospheric attenuation curves for comparison to Helliwell and explain any discrepancies. We begin by assessing the importance of various factors in trans-ionospheric attenuation, such as wave polarization, incidence angle, bearing, and the ionospheric density profile, so as to better understand and apply attenuation estimates. We then provide sets of trans-ionospheric attenuation curves that are specifically applicable to the magnetospheric injection of VLF waves from terrestrial, short, vertical dipolar radiators, representative of both Navy VLF transmitters and cloud-to-ground lightning flashes. We also provide trans-ionospheric attenuation curves for the case of a single whistler-mode wave vertically incident upon the ionosphere. Finally, we compare the FWM results to Helliwell's absorption curves and rectify any apparent incongruities found with other recent studies.

2. Model Descriptions

[8] In this work, we use three different models of trans-ionospheric attenuation: (1) the absorption curves from Figure 3-35 of *Helliwell* [1965], (2) the FWM model detailed by *Lehtinen and Inan* [2008, 2009] and utilized by *Cohen et al.* [2012], and (3) a simplified, quicker version of that FWM model that, much like *Helliwell* [1965] and the model of *Tao et al.* [2010], considers only single incident plane waves.

2.1. Helliwell's Absorption Curves

[9] The curves shown in Figure 3-35 of *Helliwell* [1965] present the total trans-ionospheric absorption of an electromagnetic whistler-mode wave through the ionosphere as a function of geomagnetic latitude. Helliwell presents four curves, specifying the absorption for 2 and 20 kHz and for daytime and nighttime. To generate the curves, he first computes the absorption as a function of wave frequency for different ionospheric conditions by numerically integrating the absorption coefficient of the wave from 60 to 1500 km altitude. Helliwell then applies multiplying factors to produce his curves of absorption as a function of geomagnetic latitude. The absorption coefficient is related to the imaginary part of the refractive index, which Helliwell calculates using the quasi-longitudinal (QL) approximation to Appleton's equations [*Ratcliffe*, 1959]. He suggests that for a 20 kHz wave, this QL approximation is valid for geomagnetic latitudes above about 25° during daytime and 45° during nighttime.

[10] Helliwell takes the incident electromagnetic wave to be whistler mode and vertically incident on either the base or top of a horizontally stratified ionosphere. He mentions that one can account for coupling effects by assuming a single sharp boundary and including the one-time reflection from

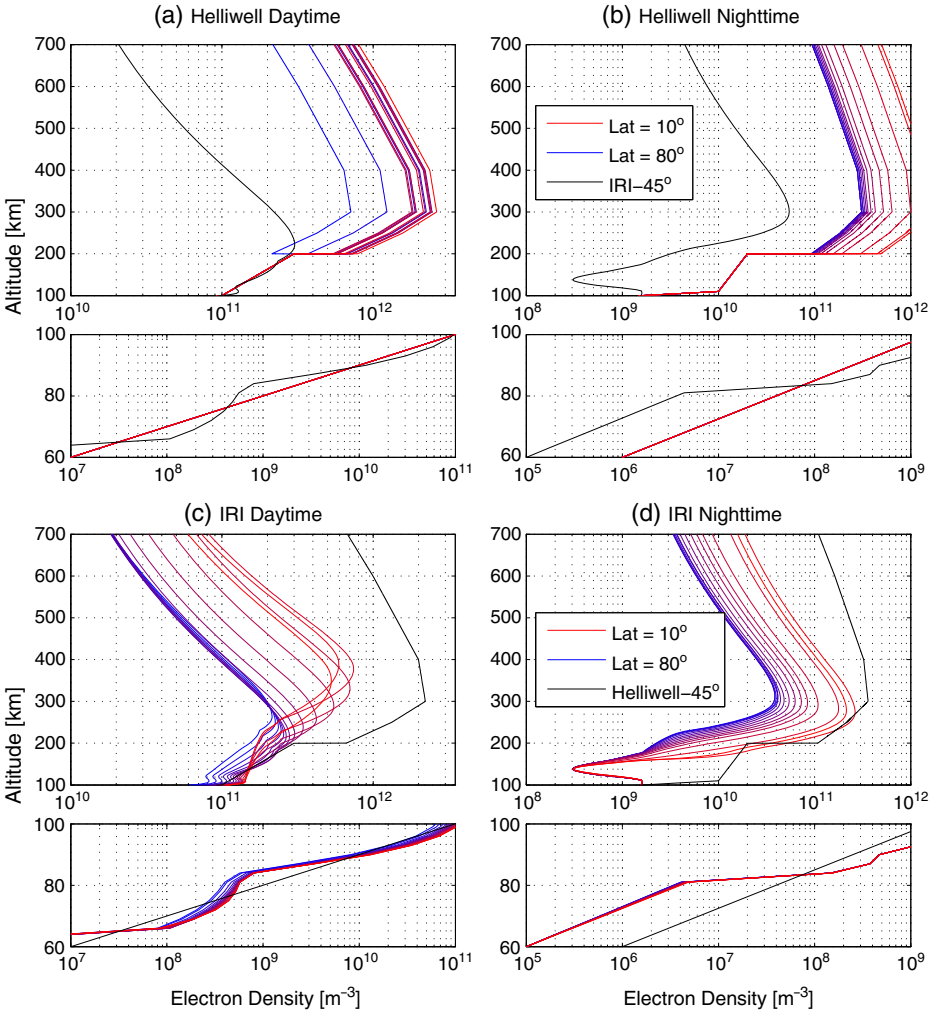

Figure 1. Electron density profiles effectively used by *Helliwell* [1965] for (a) daytime and (b) nighttime and drawn from the International Reference Ionosphere (IRI) for (c) daytime and (d) nighttime. In each panel, the electron density profile is plotted for each 5° step in latitude ranging from 10° in red to 80° in blue. To assist with comparing the IRI profiles to the Helliwell profiles, the IRI profiles for 45° latitude are included in black in Figures 1a and 1b, and the Helliwell profiles for 45° latitude are included in black in Figures 1c and 1d.

this boundary as an additional loss, but he does not include this loss in his absorption calculations. Helliwell suggests that if the incident wave is linearly polarized as opposed to whistler mode, then an additional 3 dB of attenuation should be added to his curves due to polarization mismatch between the transmitted and incident waves. Any effects due to reflection from the ground in the Earth-ionosphere waveguide are not accounted for in this model.

[11] *Tao et al.* [2010] successfully reproduces Helliwell's absorption curves by integrating the absorption coefficient for each frequency and time of day at each point in geomagnetic latitude, and we do so again here. Given this more direct approach, the media parameters specified in the computation of Helliwell's absorption curves are effectively the background magnetic field, electron density, and collision frequency. These parameters all vary with latitude. The background magnetic field is computed using a dipole model of the Earth's magnetic field. The electron density and collision frequency profiles are divided into two parts—one for the lower ionosphere (60 to 200 km altitude), which does not vary with latitude, and one for the upper ionosphere (200 to 1500 km altitude), which does vary with latitude. The collision frequency is the sum of his derived electron-neutral and electron-ion collision frequencies. The electron density and collision frequency profiles effectively used by *Helliwell* [1965] are shown in Figures 1a and 1b and Figures 2a and 2b, respectively. The corresponding profiles from the International Reference Ionosphere (IRI), which we use with the FWM model and explain in detail in the next subsection, are provided for comparison in Figures 1c and 1d and Figures 2c and 2d.

2.2. Full Wave Method (FWM)

[12] The full wave method described in *Lehtinen and Inan* [2008, 2009] is a versatile and computationally efficient modeling approach which intrinsically accounts for wave attenuation along with multiple reflections, polarizations, and incidence angles, even if the medium is not slowly

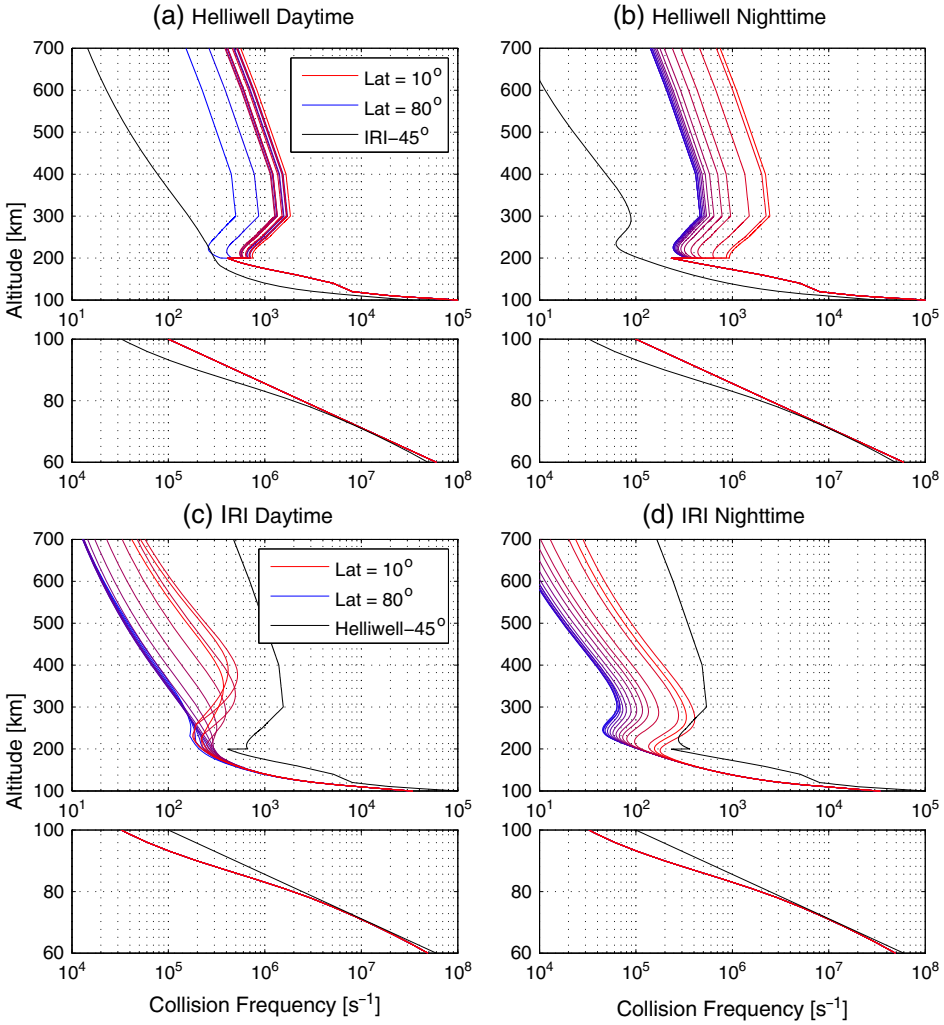

Figure 2. Collision frequency profiles effectively used by *Helliwell* [1965] for (a) daytime and (b) nighttime and as used in our FWM model for (c) daytime and (d) nighttime. In each panel, the collision frequency profile is plotted for each 5° step in latitude ranging from 10° in red to 80° in blue. To assist with comparing the IRI profiles to the Helliwell profiles, the IRI profiles for 45° latitude are included in black in Figures 2a and 2b, and the Helliwell profiles for 45° latitude are included in black in Figures 2c and 2d.

varying. For specified source current and media parameters, the field values can be computed for any horizontal plane—whether that plane is below, in, or above the ionosphere. This method assumes horizontally stratified media and solves for the reflection coefficients at each boundary in a manner that avoids the numerical "swamping" instability that is a concern for full wave method efforts [*Nygrén*, 1982]. The method was inspired by *Wait* [1970], and a detailed introduction to full wave methods can be found in *Budden* [1985, Ch. 15–19].

[13] As with Helliwell's approach, the configurable media parameters are the background magnetic field, electron density, and collision frequency. We once again compute the background magnetic field using a dipole model of the Earth's magnetic field, with the value of the field on the equator at the Earth's surface set to $B_0 = 3.12 \times 10^{-5}$ T. We specify the electron density profiles using the latest International Reference Ionosphere (IRI) model: IRI-2007 [*Bilitza and Reinisch*, 2008]. Our selected electron density profiles for each step in latitude are shown in Figures 1c and 1d for daytime and nighttime. To acquire the set of daytime profiles, we choose local noon on the date of 15 July 2009 at a geographic longitude of 0°, and we vary the latitude from 10° to 80° in 5° steps. We choose a summer month to ensure that the entire range in latitude is in daytime, and we choose the year 2009 to overlap with the lifespan of DEMETER—a satellite which has been critical to many recent studies [e.g., *Lehtinen and Inan*, 2009; *Cohen and Inan*, 2012; *Cohen et al.*, 2012]. To acquire the set of nighttime profiles, we change the month to January and the local time to midnight. Compared to Helliwell's profiles, these IRI profiles tend to show significantly lower levels of electron density. *Tao et al.* [2010] analyzed in situ electron density values measured in several rocket studies to provide statistical bounds for the *D* region electron density profiles. Based on their analysis and following the lead of *Cohen et al.* [2012], we define the IRI-2007 electron density profiles of Figures 1c and 1d as our set of "regular" profiles, and we multiply these by

5 for nighttime and 2 for daytime to estimate a "dense" ionosphere. Similarly, we divide by five for nighttime and two for daytime to estimate a "sparse" ionosphere. We use these dense, regular, and sparse profiles to study typical ionospheric variation.

[14] Similar to the approach used by Helliwell, we compute our collision frequency profiles as the sum of electron-neutral and electron-ion collisions. The electron-ion collision frequencies only add significantly to the total collision frequency above 200 km altitude, and they only add significantly to trans-ionospheric attenuation for very high electron density values in the *F* region, so their omission can often be justified. Electron-ion collisions are significant for several of Helliwell's electron density profiles, however, so we will include them in all cases here for the sake of consistency. We compute the electron-neutral collision frequency based on *Swamy* [1992], and we compute the electron-ion collisions as in *Helliwell* [1965, p. 64]. Thus, our collision frequency profiles are a function of electron density and time of day. Collision frequency profiles for each step in latitude are shown in Figures 2c and 2d for daytime and nighttime. These collision frequency profiles calculated from the IRI electron density data consistently fall below the corresponding profiles of Helliwell. If an electron density profile is modified to analyze a dense or sparse ionosphere, then the associated collision frequency profile is recalculated.

[15] In assessing the amount of power injected into the magnetosphere from a terrestrial VLF source, we model that source as a 1 MW, short, vertical dipole 1 m above the surface of a flat, conducting Earth of conductivity $\sigma = 10$ mS/m. The power above the ionosphere is computed as the upward-propagating power on a horizontal plane at 700 km altitude. We choose 700 km altitude for consistency with the DEMETER satellite observations of *Cohen and Inan* [2012] and *Cohen et al.* [2012] and with the analysis of *Starks et al.* [2008]. While Helliwell's absorption curves go all the way to 1500 km for the top of the ionosphere, the amount of attenuation between 700 km and 1500 km altitude is often negligible (this point will be discussed in more detail in section 3.) To compute the total upward-propagating power at 700 km altitude, we integrate the upward-propagating power flux in **k** space. This procedure has the advantage of accounting for all power at that altitude that is within a certain range in **k**, and this range can easily be set to capture nearly all of the power that could be radiated from our source to that altitude. Integrating the power in **r** space with the more traditional Poynting vector only captures the power within the physical **r** space limits of the simulation space. Either computation method is acceptable for a sufficiently large simulation space, but we deem the **k** space estimate to be less computationally intensive for our purposes and use it here.

2.3. Quick Full Wave Method (QFWM)

[16] The FWM model provides our most accurate estimate of the amount of power reaching a horizontal plane above the ionosphere from a specified terrestrial source. That, however, presents a very complicated picture with multiple reflections, waveguide modes, and incidence angles. For purposes of analysis, it is useful to look at simpler scenarios much like those used to produce Helliwell's absorption curves. In the QFWM model, we consider only a single plane wave incident on the base of the ionosphere. We vary the incidence angle, bearing, and polarization of this wave, along with aspects of the background media. This procedure makes for much quicker computation and, more importantly, allows us to isolate and analyze the extent to which specific factors affect trans-ionospheric attenuation. The full wave method of *Lehtinen and Inan* [2008, 2009] is still used to compute the reflection and transmission coefficients for propagation through the ionosphere. While this model considers only a single incident plane wave, we do account for the presence of multiple incoherent reflections between the Earth and the ionosphere in computing the attenuation estimate, as described in Appendix A, thereby avoiding complicated Earth-ionosphere waveguide mode interference patterns. Since the portion of the incident wave that reflects from the ionosphere can subsequently reflect from the Earth and be incident once again upon the base of the ionosphere, accounting for these multiple reflections leads to increased power injected through the ionosphere. Although such multiple reflection effects decrease the apparent attenuation, the effect on the QFWM results presented in this paper is never more than $\sim$1 dB.

3. Model Results

[17] In this section, we first use the QFWM model to illustrate the effects of several important factors for magnetospheric injection that were not accounted for in Helliwell's absorption curves. Then we use the FWM model to produce a set of trans-ionospheric attenuation curves which are more applicable to magnetospheric injection from a terrestrial VLF source. For the sake of clarity, the initial illustrative analysis will focus on the case of a 20 kHz wave penetrating through the nighttime ionosphere. Note that we use the term "attenuation" throughout to refer to the ratio of the total power which penetrates through the ionosphere to the power of the source. Thus, reflection and absorption both add to the wave attenuation in this context.

[18] We begin in Figure 3a by reproducing Helliwell's absorption curve. Helliwell's absorption curve, as read directly from Figure 3-35 of *Helliwell* [1965], is plotted in dotted black. Our recalculation of that absorption curve is plotted in dotted red for the case of a whistler-mode wave vertically incident on the base of the ionosphere, using Helliwell's ionospheric profiles and integrating the losses from 60 km to 1500 km as did Helliwell. We do not use the QL approximation in our recalculation, and we likely handle the numerical integration differently, but this approach successfully reproduces Helliwell's curve to within a few percent at all latitudes above 30°. The QL approximation is known to fail at low latitudes, thus accounting for the increased deviation below 30°. The dotted green curve shows the results of integrating to only 700 km altitude instead of to 1500 km, and the decrease in estimated attenuation is clearly very small. Since the decrease in the upper altitude limit makes such a small difference in the total attenuation, we proceed with the 700 km upper limit for consistency with the DEMETER observations of *Cohen et al.* [2012].

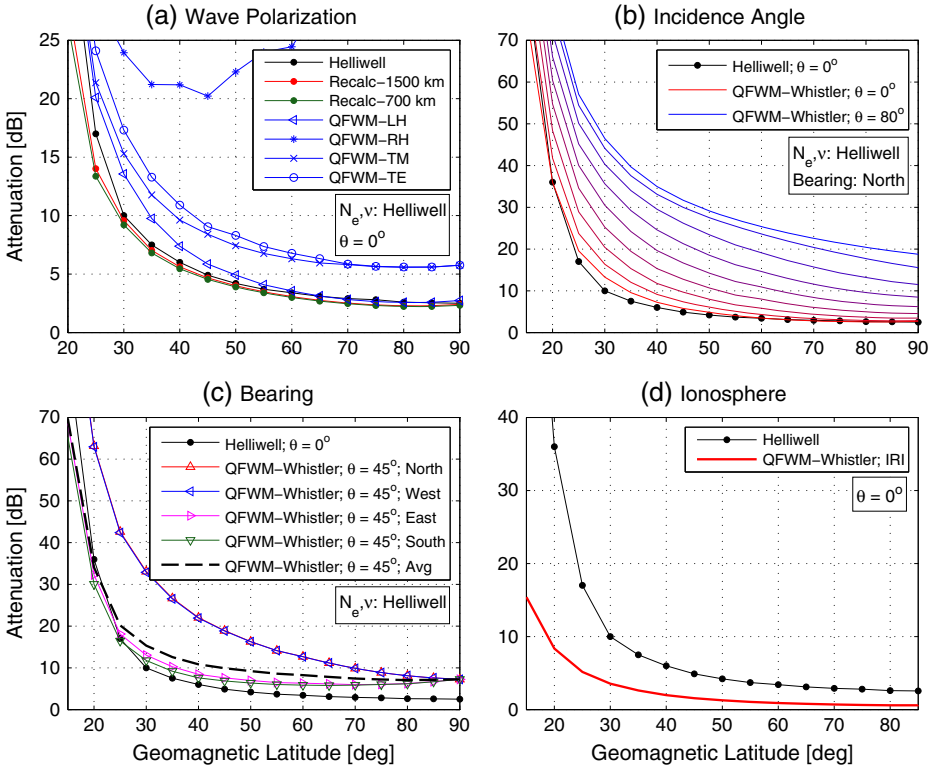

Figure 3. Illustrative QFWM results showing the importance of various factors which affect trans-ionospheric attenuation of VLF waves: (a) wave polarization, (b) incidence angle, (c) bearing, and (d) ionosphere profile. All curves are for a 20 kHz wave at nighttime. Helliwell's absorption curve is included as the dotted black curve in each panel, and our recalculation of Helliwell's absorption curve is included in Figure 3a.

[19] The four blue curves of Figure 3a show the effect of wave polarization on trans-ionospheric attenuation. We produce each of these curves using the QFWM model. The triangle- and asterisk-marked curves are for left-hand (LH) and right-hand (RH) circularly polarized waves, respectively. Traveling upward through the ionosphere in the Northern Hemisphere, LH is the whistler-mode wave, while RH is mostly evanescent. The LH curve is intended to reproduce Helliwell's absorption curve by considering a vertically incident, whistler-mode wave. The match with Helliwell's absorption curve is excellent for latitudes above 50°, but there is some deviation at lower latitudes, most likely due to the fact that the QFWM model accounts for reflections while Helliwell's absorption curves do not. The deviation there is still no more than a few decibels, but this does alert us to small potential deviations between the integration approach and the QFWM modeling approach at low latitudes. The last two blue curves in this figure show attenuation for the transverse magnetic (TM) and transverse electric (TE) modes. As Helliwell suggests, changing the incident wave from whistler mode to one of these linear polarizations leads to a ∼3 dB increase in the trans-ionospheric attenuation.

[20] In Figure 3b, we analyze the effects of changing the incidence angle of the wave impinging on the lower ionosphere. Helliwell's absorption curve is again reproduced in dotted black. The family of colored curves then illustrates the transition from vertical incidence ($\theta = 0°$) in red to grazing incidence ($\theta = 80°$) in blue. We produced this family of curves using the QFWM model, so the red ($\theta = 0°$) curve in this figure matches the QFWM-whistler curve in Figure 3a. All these curves are again produced using Helliwell's ionospheric profiles and an incident whistler-mode wave. The results show that incidence angle is a very important factor in trans-ionospheric attenuation. At 35° magnetic latitude, a grazing incidence, whistler-mode wave suffers ∼30 dB more attenuation than a vertically incident, whistler-mode wave for this bearing. Vertical incidence can be a reasonable assumption for certain cases—such as for a whistler impinging from the magnetosphere upon the top of the ionosphere at high latitudes—but several important scenarios necessitate the inclusion of higher incidence angles. For the case of radiation from a terrestrial VLF transmitter (which can be estimated as a short, vertical dipole), there is a null in the antenna radiation pattern for 0° incidence, the incident power will peak with an incidence angle around ∼45°, and the waves mostly approach grazing incidence at waveguide distances greater than ∼150 km. Since 45° incidence is a significant contributor to magnetospheric injection from terrestrial VLF transmitters and it is an appropriate midway choice between vertical and grazing incidence, we continue with analysis at this incidence angle in Figure 3c.

[21] Next, we examine the effects of changes in bearing angle by considering wave propagation in the four cardinal directions. The family of curves in Figure 3b are all for waves headed to the north. In Figure 3c, we take strictly the 45° incidence angle, but vary the bearing between north, south, east, and west. An average of those four is also provided. For these four QFWM curves and their average,

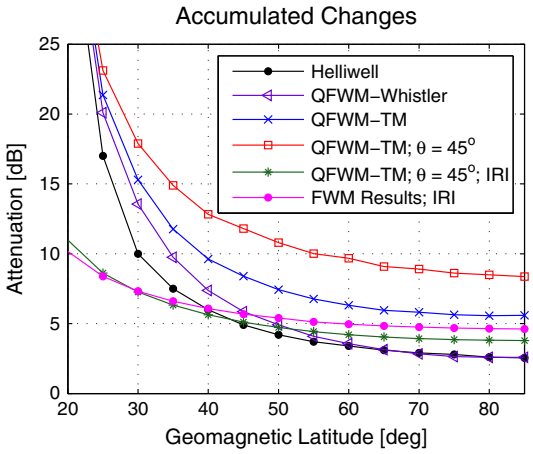

Figure 4. Accumulated changes to the trans-ionospheric attenuation of a 20 kHz wave at nighttime, illustrated using QFWM results. The effects of polarization, incidence angle and bearing, and updated ionosphere profiles are sequentially added. Also shown are Helliwell's absorption curve in dotted black and the FWM results in dotted magenta.

we again use a whistler-mode wave and Helliwell's ionospheric profiles. There is significantly more trans-ionospheric attenuation for wave propagation to the north and west. At 35° magnetic latitude, there is ∼20 dB more attenuation for a wave headed to the north as opposed to the south. The average over the four cardinal directions provides a rough attenuation estimate if all bearing angles are to be accounted for equally.

[22] Finally, in Figure 3d, we show the effect of changing the ionospheric profile from Helliwell's values to the set of IRI-2007 values for both electron density and collision frequency. For better comparison to Helliwell's absorption curve in this figure, we return to considering a whistler-mode wave vertically incident upon the ionosphere. As expected, the lower electron density and collision rates of the IRI-2007 profiles lead to a significant decrease in attenuation. This result is clear despite the tendency of the QFWM-whistler result to estimate slightly more attenuation at low latitudes compared to Helliwell's absorption curves (as we showed in Figure 3a for both curves using Helliwell's ionospheric profiles). For this case of a 20 kHz, whistler-mode wave vertically incident upon a nighttime ionosphere, the switch to the IRI-2007 ionospheric profiles estimates ∼30–40% less attenuation outside of the equatorial region. This is similar to the change shown by *Tao et al.* [2010] for a transition from Helliwell's ionospheric profiles to the IRI.

[23] In Figure 4, we accumulate each of the changes we just analyzed in Figure 3 as we move toward the FWM results. Helliwell's absorption curve is reproduced again in dotted black, and the vertically incident QFWM-whistler in purple is provided again as this model's closest reproduction of Helliwell's result. This is using whistler-mode, vertical incidence, and Helliwell's ionospheric profiles. Moving to the blue QFWM-TM curve, we see the effect of switching

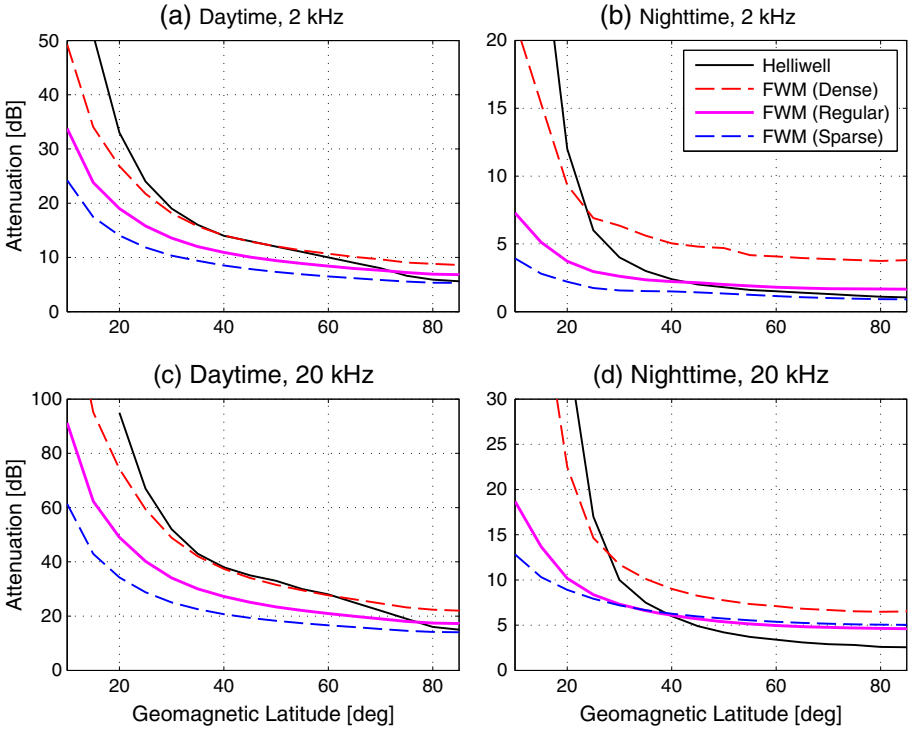

Figure 5. Estimates of trans-ionospheric attenuation of VLF waves as calculated using the FWM model. Results are provided for (a) daytime, 2 kHz; (b) nighttime, 2 kHz; (c) daytime, 20 kHz; and (d) nighttime, 20 kHz. Dense (×2 daytime, ×5 nighttime), regular (see Figures 1c, 1d, 2c, and 2d), and sparse (÷2 daytime, ÷5 nighttime) ionospheres are considered for each case. These results are most applicable to estimating the total magnetospheric injection from a terrestrial VLF source. Helliwell's absorption curves are included for reference.

from an incident whistler-mode wave to an incident linearly polarized wave: ∼3 dB increase in attenuation due to the nonwhistler-mode, circularly polarized component being evanescent in the ionosphere. Moving to the red curve, we keep the TM polarization and shift from vertical incidence to a 45° incidence angle. To account for bearing here, we provide only the average of the four cardinal directions. This change again adds several decibels of attenuation across all latitudes. Finally, we take this scenario and switch the ionospheric profiles from Helliwell's to the IRI-2007 set for both electron density and collision frequency. The result is a substantial decrease in the attenuation estimates, producing the final QFWM curve in green which predicts less attenuation at low latitudes, and slightly more at high latitudes, compared to Helliwell's absorption curve. One additional curve is provided in this figure: the FWM results are shown with the dotted magenta curve. The FWM results, which consider the more complicated picture of radiation from a terrestrial source as opposed to considering only single incident plane waves like in the QFWM, provide our most accurate attenuation estimate for the total amount of power penetrating through the ionosphere from a specified terrestrial source. We note that the final QFWM result plotted in green agrees closely with the FWM for this case. The choices of TM polarization, 45° incidence, averaging over the four cardinal directions, and using the IRI-2007 ionospheric profiles are chosen to roughly mimic the case of magnetospheric injection from a terrestrial VLF transmitter.

[24] Having assessed the importance of various factors in the trans-ionospheric attenuation of VLF waves, we provide the set of FWM attenuation curves in Figure 5. We generate these curves using the FWM model for a short, vertical dipole radiating 1 MW of power at 2 or 20 kHz near the surface of a flat, conducting Earth of conductivity σ = 10 mS/m, as was described in section 2.2. We provide both Helliwell's absorption curves and our FWM results for 2 kHz and 20 kHz and for daytime and nighttime. We consider dense, regular, and sparse ionospheres (as defined in section 2.2) for each FWM result. Both Helliwell and FWM predict significantly more attenuation at lower latitudes, but the effect is less pronounced in the FWM results; in comparison to Helliwell, FWM predicts less attenuation at low latitudes and more attenuation at high latitudes. While the discrepancy between the models grows large in the equatorial region where attenuation is high, Helliwell and FWM agree to within ∼10 dB for latitudes greater than 35° for daytime, and they agree to within ∼5 dB for latitudes greater than 30° for nighttime. The FWM daytime ionospheric variation shows a spread of ±3–4 dB at midlatitudes for 2 kHz and ±5–8 dB at midlatitudes for 20 kHz. The FWM nighttime ionospheric variation shows less than 1 dB of change in attenuation between the regular and sparse ionospheres, but the dense ionosphere adds 2–4 dB for both 2 kHz and 20 kHz at midlatitudes.

[25] Dry-Earth conductivity typically varies between 3 and 30 mS/m, so our ground conductivity of 10 mS/m is a reasonable estimate for much of the nonpolar land on Earth. However, sea water is ∼4–5 S/m, icy regions are only ∼0.01–0.1 mS/m, and localized mineral deposits or sediment composition can lead to further variations [*Morgan*, 1968]. Figure 6 compares the FWM results for two different values of ground conductivity: the 10 mS/m used to generate the FWM results of Figure 5 and the 0.1 mS/m used by *Cohen et al.* [2012]. We use only the regular ionosphere profiles for this analysis. The change in ground conductivity from 10 mS/m to 0.1 mS/m has very little effect on trans-ionospheric attenuation for a 2 kHz source, but for 20 kHz, it adds ∼1.5 dB attenuation to the daytime curve and ∼2.5 dB to the nighttime curve.

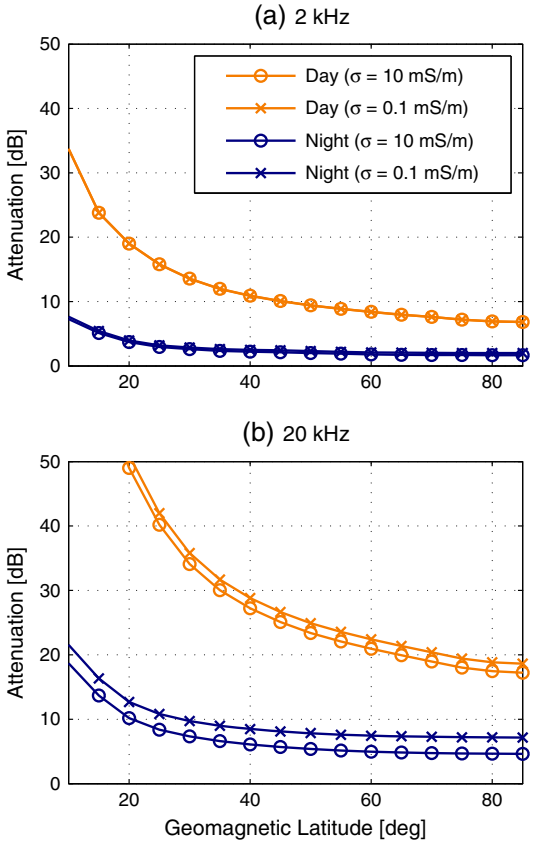

Figure 6. Comparison of FWM trans-ionospheric attenuation estimates for different values of ground conductivity. Results are provided for (a) 2 kHz and (b) 20 kHz, and for daytime (orange) and nighttime (blue). Results for σ = 0.1 mS/m are marked with circles, and results for σ = 10 mS/m are marked with x's. We use the ionosphere profiles of Figures 1c, 1d, 2c, and 2d for each curve.

[26] Just as Helliwell's absorption curves, the FWM results of Figure 5 only provide trans-ionospheric attenuation estimates for a specific scenario. In the scenario for Figure 5, the waves incident on the base of the ionosphere as radiated by a short, vertical, dipolar terrestrial VLF source are composed of many polarizations and incidence angles. A null exists in the antenna radiation pattern for vertical (0°) incidence, and the power incident on the base of the ionosphere peaks for an incidence angle around 45°. To consider an alternate scenario that more directly updates Helliwell's absorption curves, Figure 7 provides trans-ionospheric attenuation estimates for the case of a whistler-mode plane wave vertically incident upon the ionosphere. These curves are meant to mimic the scenario used for Helliwell's absorption curves, but simply update them with the IRI-2007 ionospheric profiles, include the effect of reflections, and remove any simplifying analytical

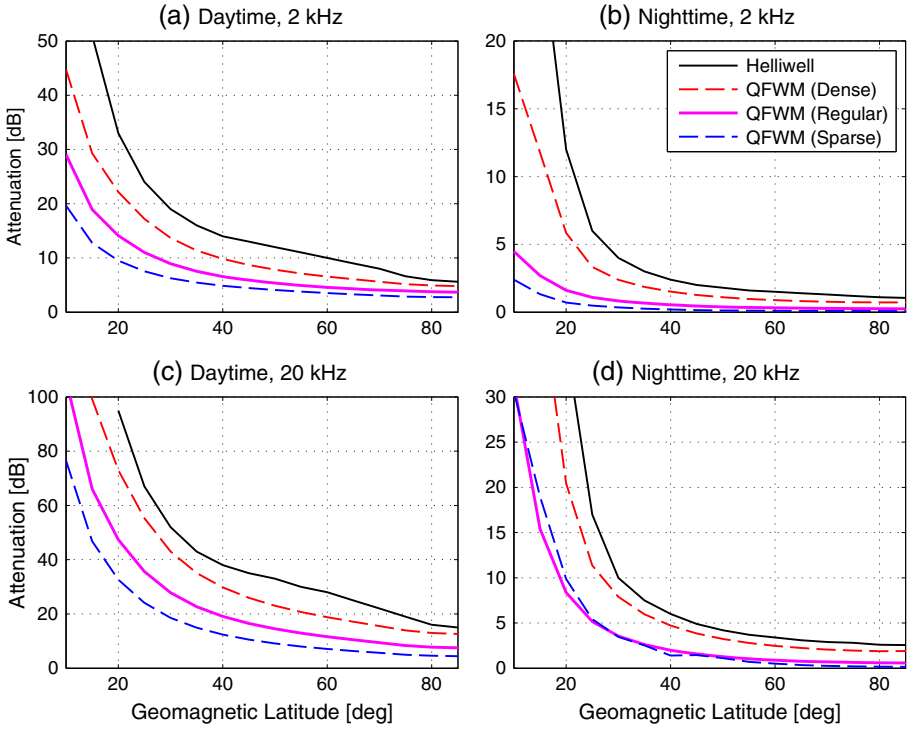

Figure 7. Estimates of trans-ionospheric attenuation of a VLF whistler-mode plane wave vertically incident upon the ionosphere. Results are provided for (a) daytime, 2 kHz; (b) nighttime, 2 kHz; (c) daytime, 20 kHz; and (d) nighttime, 20 kHz. Dense (×2 daytime, ×5 nighttime), regular (see Figures 1c, 1d, 2c, and 2d), and sparse (÷2 daytime, ÷5 nighttime) ionospheres are considered for each case. Helliwell's absorption curves are included for reference.

approximations. The change in ionospheric profiles leads to a significant decrease in attenuation estimates compared to Helliwell, as we would expect. One potential application of these curves is that, in many cases, they should provide reasonable trans-ionospheric attenuation estimates for the case of whistler-mode plane waves penetrating from the magnetosphere, through the ionosphere, and into the Earth-ionosphere waveguide. Many of those waves will propagate approximately along the Earth's magnetic field while in the magnetosphere. Whether such a whistler-mode wave is incident vertically or approximately field-aligned, the trans-ionospheric attenuation estimates remain very close to those provided in Figure 7 as long as the wave normal is within the cone of transmission at the ionospheric boundary [*Helliwell*, 1965, section 3.7]. This result is tied to our bearing angle analysis. If the bearing is such as to align the whistler-mode wave along the background magnetic field as opposed to across it, then the resulting attenuation is nearly the same as for vertical incidence.

4. Discussion

[27] *Cohen et al.* [2012] thoroughly compared the FWM model to the average of thousands of DEMETER satellite passes for magnetospheric injection from ∼20 kHz terrestrial VLF transmitters, finding agreement to within ±6 dB between model and observation for every transmitter analyzed, and for both daytime and nighttime. To properly compare with DEMETER observations, *Cohen et al.* [2012] utilized specific ionosphere profiles and transmitter parameters in the FWM model for optimal comparison to each VLF transmitter. They also integrated the power above the ionosphere computed by the FWM model in **r** space using the same integration technique as applied to DEMETER data in *Cohen and Inan* [2012]. Their analysis served to validate the FWM model as a means of predicting magnetospheric injection from terrestrial VLF transmitters. The simulations utilized here are identical, apart from our use of more general ionosphere profiles and transmitter frequencies, integration in **k** space to compute total power, and our use of a more realistic ground conductivity of 10 mS/m as opposed to 0.1 mS/m. The impact of this ground conductivity change on the results is 1–2 dB, which actually brings the FWM model results of *Cohen et al.* [2012, Figure 4] into even closer alignment (±5 dB) with the DEMETER observations.

[28] While *Cohen et al.* [2012] validated the FWM model for frequencies around 20 kHz, validation for the 2 kHz range is more difficult as there are no VLF transmitters operating in that frequency range. The best approach is to use natural lightning, which emits energy across the whole ELF/VLF spectrum. This comparison of the FWM model to observation for magnetospheric injection from a lower frequency terrestrial source is ongoing. At this point in time, the FWM model is not yet experimentally validated at 2 kHz for our specific application of estimating trans-ionospheric attenuation. We also note that *Cohen et al.* [2012] focus their comparisons at midlatitudes, with no observations made below 20° magnetic latitude or above 65° magnetic latitude. In other words, the results in the equatorial and polar

regions are not currently validated by observations. Low-latitude whistlers observed on the ground [*Singh et al.*, 2012] may provide a future technique to experimentally validate the low-latitude absorption models. We have no reason to believe the FWM approach will fail at lower frequencies or at equatorial or polar latitudes, however, and the method has been successfully applied in the 1 to 3 kHz frequency range in previous studies for related applications [e.g., *Piddyachiy et al.*, 2008; *Cohen et al.*, 2010].

[29] With the FWM model validated to within ±6 dB by *Cohen et al.* [2012] for ∼20 kHz emissions from terrestrial VLF transmitters, the set of curves presented in Figure 5 provides our most accurate estimate of trans-ionospheric attenuation using a generic set of ionospheric profiles and transmitter parameters. These provide our best estimate of trans-ionospheric attenuation for the case of total power injected into the magnetosphere from a short, vertical, monochromatic, terrestrial VLF source. The remaining ∼5–6 dB of error observed by *Cohen et al.* [2012] may be due to ionospheric variation and/or physical limitations of our FWM model. Since the medium in our FWM model is horizontally stratified, scattering from field-aligned irregularities or coupling into quasi-electrostatic modes [*Bell and Ngo*, 1990] is not accounted for, and this phenomenon could add to the trans-ionospheric attenuation of VLF waves [*Foust et al.*, 2010; *Bell et al.*, 2011; *Shao et al.*, 2012]. Both *Shao et al.* [2012] and *Foust et al.* [2010] can attribute several decibels of additional attenuation to the interaction of VLF waves with field-aligned irregularities, and both suggest that effect is more likely to occur during nighttime. The FWM does not account for such irregularities, so although *Cohen et al.* [2012] significantly downplayed the global role of irregularities, both naturally present and especially generated by the VLF heating, it is possible that a few decibels of attenuation should be added to our estimates for nighttime, 20 kHz at midlatitudes. The same may also be true for 2 kHz. Additionally, a persistent ∼20% reduction in electron density near 80 km altitude may exist overhead a powerful VLF transmitter due to the ionospheric heating induced by the transmitter itself [*Rodriguez and Inan*, 1994]. This amount of deviation is captured by our ionospheric variation analysis, but a persistent increase in electron temperature and reduction in electron density could affect our estimate of typical trans-ionospheric attenuation.

[30] Comparison of the QFWM and FWM models appears capable of rectifying the disparate conclusions of *Starks et al.* [2008], *Tao et al.* [2010], and *Cohen et al.* [2012] with regards to trans-ionospheric absorption. For 20 kHz, daytime at midlatitudes, *Starks et al.* [2008] suggests that ∼10 dB more attenuation needs to be added to Helliwell's absorption curves to bring it into line with observations. The results of *Cohen et al.* [2012] suggest ∼10 dB less attenuation is needed in this scenario, not more. The FWM results presented in Figure 5c agree with the DEMETER observations of *Cohen et al.* [2012] and thus disagree with the conclusions of *Starks et al.* [2008]. The discrepancy is due to amount of data analyzed and incidence angle.

[31] The data presented by *Cohen and Inan* [2012] are based on hundreds of satellite passes over each of a dozen different terrestrial VLF transmitters, facilitating the creation of a 25 km resolution map of each transmitter's radiation pattern at 700 km altitude. The observations of *Starks et al.* [2008] consist of no more than 16 satellite passes over any given VLF transmitter. *Cohen and Inan* [2012] simply analyze much more data, providing better averaging over ionospheric variation and a better view of the center of the radiation pattern where the bulk of the VLF energy is found.

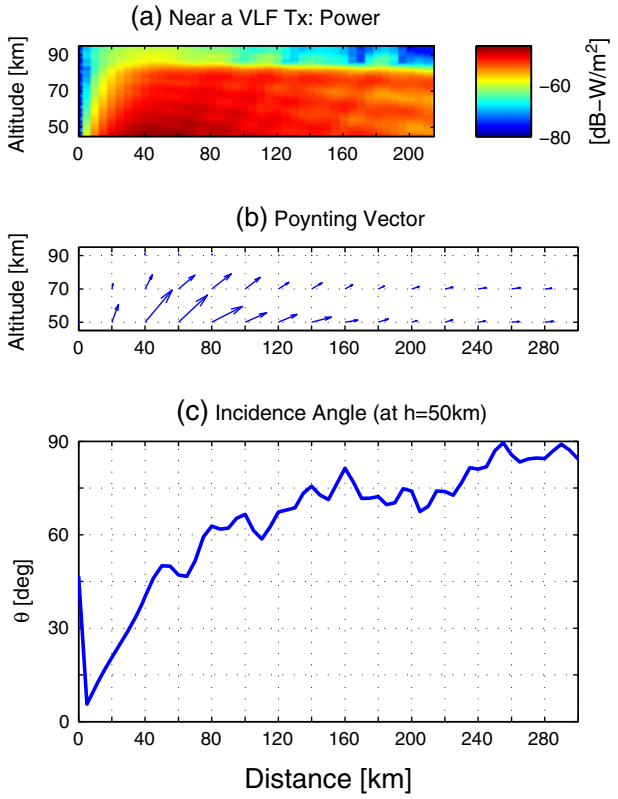

Figure 8. (a) Illustrative FWM results depicting (b) the direction and relative magnitude of the Poynting vector near the base of the ionosphere in the vicinity of a terrestrial VLF transmitter. (c) The estimated wave incidence angle, which very quickly approaches grazing incidence as the wave progresses forward in the Earth-ionosphere waveguide.

[32] It is clear from the radiation patterns of *Cohen and Inan* [2012] and *Cohen et al.* [2012] that if a satellite pass is not within ∼150 km of the center of the radiation pattern, then the bulk of the peak power injected into the magnetosphere will not be observed. *Starks et al.* [2008], following the procedure developed by *Inan et al.* [1984], partially accounted for this fact by properly scaling the power of the VLF waves injected into the base of the ionosphere. However, *Inan et al.* (and, by extension, *Starks et al.*) did not account for change in incidence angle; they applied Helliwell's absorption curves to estimate the trans-ionospheric attenuation at each point, which is equivalent to assuming vertical incidence at all points. As was shown in Figure 3b, changing from vertical incidence to grazing incidence causes a significant increase in trans-ionospheric attenuation (decrease in magnetospheric injection). In Figure 8, we use FWM results to analyze the wave incidence angle moving away from a terrestrial VLF transmitter. In the top panel, we provide the computed wave

power density for within 300 km horizontal distance of a transmitter over an altitude range covering the base of the ionosphere. In the middle panel, we plot the Poynting vector for these results, computed as the cross-product of the total electric and magnetic fields at each point. The angle between this Poynting vector at 50 km altitude and vertical provides the incidence angle estimate plotted in the bottom panel. While this estimate of incidence angle does not fully account for the presence of multiple modes which each possess their own power and incidence angle, it should capture the effects of the dominant modes for this analysis. The Poynting vector shows a maximum for $\sim$45° incidence angle, and the waves approach grazing incidence very quickly as they progress forward in the Earth-ionosphere waveguide. For waves penetrating the ionosphere even $\sim$150 km from the transmitter, the Helliwell absorption curves will grossly underestimate the trans-ionospheric attenuation. If most of the satellite passes analyzed by *Starks et al.* [2008] were more than $\sim$150 km horizontal distance ($\sim$1.3°) away from the center of the specified VLF transmitter's radiation pattern, then direct use of Helliwell's absorption curves to estimate trans-ionospheric attenuation would lead to the discrepancies between *Starks et al.* [2008] and *Cohen et al.* [2012].

[33] *Tao et al.* [2010] present results from their own full wave method to study the variance of trans-ionospheric attenuation with changes in background electron density. Similar to our results in Figures 3d and 7, they find trans-ionospheric attenuation to be strongly dependent on the electron density of the ionosphere and analyze this particular phenomenon in more depth than done here. As both we and *Tao et al.* [2010] conclude, the media profiles used by *Helliwell* [1965] mostly overestimate the ionospheric electron density, and updating these profiles to more recent models leads to a substantial decrease in the estimated trans-ionospheric attenuation. *Tao et al.* [2010], however, look strictly at single plane waves incident vertically on the base of the ionosphere. This led to the apparent discrepancy with the results of *Starks et al.* [2008], where the conclusions of *Tao et al.* [2010] were again mostly suggesting less attenuation than Helliwell as opposed to more. As we discussed above, the effect of incidence angle is likely significant enough in this scenario to reconcile the incongruity.

5. Conclusion

[34] Helliwell's curves provide exactly what they claim: estimates of trans-ionospheric absorption for a whistler-mode plane wave vertically incident upon the base of a specified ionosphere, with the values incurring some error at low latitudes where the QL approximation is invalid. The ionospheric profiles used by Helliwell should be updated to contemporary models (as we did here for Figure 7), but otherwise his approach appears valid for the stated intentions. However, the Helliwell curves are not well applicable to estimate the magnetospheric injection of waves from a short, dipolar, terrestrial transmitter. Incidence angle, bearing, wave polarization, multiple reflections, and ionospheric variation all affect that situation in ways not fully captured by Helliwell's approach.

[35] The new set of curves presented here in Figure 5 provide estimates of trans-ionospheric attenuation for the total amount of power injected into the magnetosphere from a terrestrial VLF transmitter. We generated these curves using the same FWM model which *Cohen et al.* [2012] shows agrees to within $\pm$6 dB of satellite-based observations for this application. We must underscore the impact of ionospheric variation and its ability to vary these results. As *Tao et al.* [2010] and *Cohen et al.* [2012] have also shown, ionospheric variation has a significant effect on trans-ionospheric attenuation. Given how difficult it is to accurately determine the electron density profile of the ionosphere for any specific time and location, and given how much the profiles may vary, applying these results to any single observation should be done with great care. Applying them to long-term averages, however, should be more effective.

[36] One of the goals of this work is to contribute to a complete understanding of the role terrestrial sources play in scattering magnetospheric electrons, particularly in the slot region [e.g., *Abel and Thorne*, 1998a, b; *Kim et al.*, 2011]. *Abel and Thorne* utilized Helliwell's trans-ionospheric absorption curves to estimate the effects of terrestrial VLF transmitters, and *Kim et al.* [2011] chose to scale the transmitter wave power in the magnetosphere down by a factor of 10 in comparison to *Abel and Thorne* based on the findings of *Starks et al.* [2008]. The FWM results of Figure 5 indicate that this factor of 10 adjustment made by *Kim et al.* [2011] may have been unwarranted. For daytime, 20 kHz, Helliwell actually overestimates the attenuation by 5–20 dB between 30° and 60° geomagnetic latitude, with greater overestimation at low latitudes. For nighttime, 20 kHz, Helliwell underestimates the attenuation at midlatitudes (30°–60°) by 0–9 dB and overestimates the attenuation at low latitudes ($\leq$20°) by 20–100 dB. Overall, these results suggest that the magnetospheric injection from terrestrial VLF transmitters at midlatitudes for nighttime does not need to be drastically adjusted from the values predicted by Helliwell's curves and utilized by *Abel and Thorne* [1998a]. Several decibels of adjustments may be necessary, but not the factor of 10 or more suggested by recent studies [*Starks et al.*, 2008; *Kim et al.*, 2011].

[37] While the trans-ionospheric attenuation curves in Figure 5 provide reasonable estimates for calculating the total power injected into the magnetosphere from a terrestrial VLF source, the analysis accompanying Figures 3, 4, and 6 highlights how limited the applicability of any single family of trans-ionospheric attenuation curves can be. Any changes to ionospheric density profile or ground conductivity affect the results. Any scenario in which the source is not a short, vertical dipole near the ground or any scenario in which incident plane waves must be analyzed individually requires the consideration of specific incidence angles, bearings, and wave polarizations.

Appendix A: Incoherent Summation of Multiply Reflected Waves

[38] The QFWM model described in section 2.3 considers single plane waves incident on the base of a horizontally stratified ionosphere, and we account for the presence of multiple incoherent reflections between the Earth and the ionosphere in computing the attenuation estimate. Let us use notations similar to *Lehtinen and Inan* [2008] and denote upward-propagating wave amplitudes below and above a layer of ionosphere in consideration (i.e., "incident"

and "transmitted" waves) as $\mathbf{u}$ and $\mathbf{u}_t$ and downward-propagating wave amplitude below ionosphere (i.e., the "reflected" wave) as $\mathbf{d}$ (all u and d are vectors of length two). For a single interaction with the ionosphere, i.e., disregarding the reflection from the ground, the transmitted and reflected waves are obtained from the incident wave using the transmission and reflection coefficients (2×2 matrices) U and R^u:

$$\mathbf{u}_t = \mathrm{U}\mathbf{u} \quad \mathbf{d} = \mathrm{R}^u\mathbf{u}_i$$

The total transmission coefficient U for a stratified ionosphere consisting of N layers is calculated from individual layer transmission coefficients U_k as $\mathrm{U} = \mathrm{U}_N\mathrm{U}_{N-1}\ldots\mathrm{U}_1$, with U_k obtained as shown in *Lehtinen and Inan* [2008]; and the reflection coefficient R^u is calculated at the lower boundary of ionosphere.

[39] The upward power flux (contained in the upward wave only) may be represented as a bilinear form

$$S = \mathbf{u}^H\mathrm{S}\mathbf{u}$$

with $\mathbf{u}^H$ being the Hermitian conjugate and S a 2×2 matrix. In general, it is different below and above the ionosphere and therefore will be denoted as $\mathrm{S}_{\mathrm{below,above}}$.

[40] Let us assume that a VLF transmitter generates an upward wave of amplitude $\mathbf{u}^0$. The absorption A in decibels is defined as

$$A = 10\log_{10}\frac{S_t}{S_i}$$

where $S_i = (\mathbf{u}^0)^H\mathrm{S}_{\mathrm{below}}\mathbf{u}^0$ is the incident vertical power flux and

$$S_t = \mathbf{u}_t^H\mathrm{S}_{\mathrm{above}}\mathbf{u}_t \tag{A1}$$

is the total transmitted vertical power flux. We cannot simply assume $\mathbf{u}_t = \mathrm{U}\mathbf{u}_0$ because this neglects waves which are multiply reflected from the ground and therefore overestimates the total attenuation. Instead, we have

$$\mathbf{u}_t = \mathbf{u}_t^0 + \mathbf{u}_t^1 + \ldots$$

where the additional terms $\mathbf{u}_t^k = \mathrm{U}\mathbf{u}^k$ are from waves that are multiply reflected from the ground, i.e. $\mathbf{u}^1 = \mathrm{R}^d\mathbf{d}^0 = \mathrm{R}^d\mathrm{R}^u\mathbf{u}^0$ is a singly reflected wave; $\mathbf{u}^n = \mathrm{R}^d\mathrm{R}^u\mathbf{u}^{n-1}$ is the wave reflected n times. Here, $\mathrm{R}^d = \mathrm{R}_g e^{i\phi}$ is the reflection coefficient from the ground, which is calculated at the altitude of the lower boundary of the ionosphere and therefore takes into account the phase change ϕ due to propagation through the space between the Earth and ionosphere. At the zero altitude, the reflection coefficient is $\mathrm{R}_g = -1$ [*Lehtinen and Inan*, 2008]. The phase change ϕ depends on the height of the ionosphere and on the angle of incidence and, if calculated exactly, is responsible for peaks and troughs in the total absorption due to interference between different multiply reflected waves $\mathbf{u}_t^n$.

[41] We take an approach which gives a better comparison with Helliwell's curves by assuming that multiply reflected waves are not coherent with each other, which may be obtained by assuming that ϕ is random and uniformly distributed in interval $[0, 2\pi]$. We have

$$\mathbf{u}_t^n = e^{in\phi}\mathrm{U}(\mathrm{R}_g\mathrm{R}^u)^n\mathbf{u}^0$$

The upward-propagating power flux, averaged over ϕ, is obtained by substituting the summed $\mathbf{u}_t$ into (A1):

$$\langle S_t\rangle_\phi = (\mathbf{u}^0)^H\mathrm{X}\mathbf{u}^0$$

where

$$\mathrm{X} = \sum_{n=0}^{\infty}\mathrm{A}^n\mathrm{B}\mathrm{C}^n$$

where we denoted for brevity $\mathrm{C} = \mathrm{R}_g\mathrm{R}^u$, $\mathrm{B} = \mathrm{U}^H\mathrm{S}_{\mathrm{above}}\mathrm{U}$ and $\mathrm{A} = \mathrm{C}^H$. The sum may be calculated (assuming it converges) by solving the linear equation for X:

$$\mathrm{X} - \mathrm{A}\mathrm{X}\mathrm{C} = \mathrm{B}$$

which is easily verified by substituting.

[42] **Acknowledgments.** This work has been supported by AFRL contract FA9453-11-C-0011 and NSF awards 1043442 and 1141791 to Stanford University. We thank Michael Starks for helpful discussions throughout, and we thank Drew Compston for discussions concerning the comparisons to lightning observations.

References

Abel, B., and R. M. Thorne (1998a), Electron scattering loss in Earth's inner magnetosphere—1. Dominant physical processes, *J. Geophys. Res.*, *103* (A2), 2385–2396.

Abel, B., and R. M. Thorne (1998b), Electron scattering loss in Earth's inner magnetosphere—2. Sensitivity to model parameters, *J. Geophys. Res.*, *103*(A2), 2397–2407.

Bell, T. F., and H. D. Ngo (1990), Electrostatic lower hybrid waves excited by electromagnetic whistler mode waves scattering from planar magnetic-field aligned plasma density irregularities, *J. Geophys. Res.*, *95*(A1), 149–172.

Bell, T. F., U. S. Inan, D. Piddyachiy, P. Kulkarni, and M. Parrot (2008), Effects of plasma density irregularities on the pitch angle scattering of radiation belt electrons by signals from ground based VLF transmitters, *Geophys. Res. Lett.*, *35*, L19103, doi10.1029/2008GL034834.

Bell, T. F., K. L. Graf, U. S. Inan, D. Piddyachiy, and M. Parrot (2011), DEMETER observations of ionospheric heating by powerful VLF transmitters, *Geophys. Res. Lett.*, *38*, L11103, doi10.1029/2011GL047503.

Bilitza, D., and B. W. Reinisch (2008), International reference ionosphere 2007: Improvements and new parameters, *Adv. Space Res.*, *42*, 599–609, doi10.1016/j.asr.2007.07.048.

Bortnik, J., U. S. Inan, and T. F. Bell (2002), *L* dependence of energetic electron precipitation driven by magnetospherically reflecting whistler waves, *J. Geophys. Res.*, *107*(A8), doi10.1029/2001JA000303.

Budden, K. G. (1985), *The Propagation of Radio Waves: The Theory of Radio Waves of Low Power in the Ionosphere and Magnetosphere*, Cambridge University Press, Cambridge, U.K.

Carpenter, D. L. (1966), Whistler studies of the plasmapause in the magnetosphere: 1. Temporal variations in the position of the knee and some evidence on plasma motions near the knee, *J. Geophys. Res.*, *71*, 693–709.

Carpenter, D. L., R. R. Anderson, T. F. Bell, and T. R. Miller (1981), A comparison of equatorial electron densities measured by whistlers and by a satellite radio technique, *Geophys. Res. Lett.*, *8*(1107).

Cohen, M. B., and U. S. Inan (2012), Terrestrial VLF transmitter injection into the magnetosphere, *J. Geophys. Res.*, *117*, A08310, doi10.1029/2012JA017992.

Cohen, M. B., U. S. Inan, M. Golkowski, and N. G. Lehtinen (2010), On the generation of ELF/VLF waves for long-distance propagation via steerable HF heating of the lower ionosphere, *J. Geophys. Res.*, *115*, A07322, doi10.1029/2009JA015170.

Cohen, M. B., N. G. Lehtinen, and U. S. Inan (2012), Models of ionospheric VLF absorption of powerful ground-based transmitters, *Geophys. Res. Lett.*, *39*, L24101, doi10.1029/2012GL054437.

Crary, J. H. (1961), The effect of the earth-ionosphere waveguide on whistlers, *Tech. Rep. 9*, Stanford Univ. Electron. Lab., Stanford, Calif.

Foust, F. R., U. S. Inan, T. F. Bell, and N. G. Lehtinen (2010), Quasi-electrostatic whistler mode wave excitation by linear scattering of EM whistler mode waves from magnetic field-aligned density irregularities, *J. Geophys. Res.*, *115*, A11310, doi10.1029/2010JA015850.

Golden, D. I., M. Spasojevic, F. R. Foust, N. G. Lehtinen, N. P. Meredith, and U. S. Inan (2010), Role of the plasmapause in dictating the ground accessibility of ELF/VLF chorus, *J. Geophys. Res.*, *115*, A11211, doi10.1029/2010JA015955.

Golden, D. I., M. Spasojevic, and U. S. Inan (2011), Determination of solar cycle variations of midlatitude ELF/VLF chorus and hiss via automated signal detection, *J. Geophys. Res.*, *116*, A03225, doi10.1029/2010JA016193.

Helliwell, R. A. (1965), *Whistlers and Related Ionospheric Phenomena*, Stanford University Press, Stanford, Calif.

Horne, R. B., et al. (2005), Wave acceleration of electrons in the Van Allen radiation belts, *Nature*, *437*, 227–230, doi10.1038/nature03939.

Imhof, W. L., et al. (1983), Direct observation of radiation belt electrons precipitated by controlled injection of VLF signals from a ground-based transmitter, *Geophys. Res. Lett.*, *10*(4), 361–364.

Inan, U. S. (1987), Gyroresonant pitch angle scattering by coherent and incoherent whistler mode waves in the magnetosphere, *J. Geophys. Res.*, *92*(A1), 127–142.

Inan, U. S., H. C. Chang, and R. A. Helliwell (1984), Electron precipitation zones around major ground-based VLF signal sources, *J. Geophys. Res.*, *89*(A5), 2891–2906.

Kim, K.-C., Y. Shprits, D. Subbotin, and B. Ni (2011), Understanding the dynamic evolution of the relativistic electron slot region including radial and pitch angle diffusion, *J. Geophys. Res.*, *116*, A10214, doi10.1029/2011JA016684.

Kulkarni, P., U. S. Inan, T. F. Bell, and J. Bortnik (2008), Precipitation signatures of ground-based VLF transmitters, *J. Geophys. Res.*, *113*, A07214, doi10.1029/2007JA012569.

Lehtinen, N. G., and U. S. Inan (2008), Radiation of ELF/VLF waves by harmonically varying currents into a stratified ionosphere with application to radiation by a modulated electrojet, *J. Geophys. Res.*, *113*, A06301, doi10.1029/2007JA012911.

Lehtinen, N. G., and U. S. Inan (2009), Full-wave modeling of transionospheric propagation of VLF waves, *Geophys. Res. Lett.*, *36*, L03104, doi10.1029/2008GL036535.

Lichtenberger, J. (2009), A new whistler inversion method, *J. Geophys. Res.*, *114*, A07222, doi10.1029/2008JA013799.

Lichtenberger, J., C. Ferencz, L. Bodnar, D. Hamar, and P. Steinbach (2008), Automatic whistler detector and analyzer system: Automatic whistler detector, *J. Geophys. Res.*, *113*, A12201, doi10.1029/2008JA013467.

Morgan, R. R. (1968), Preparation of a world wide VLF effective conductivity map, *Tech. Rep. AD0669917*, Westinghouse Electric Corp Environmental Science and Technology Dept.

Nygrén, T. (1982), A method of full wave analysis with improved stability, *Planet. Space Sci.*, *30*(4), 427–430, doi10.1016/0032-0633(82)90048-4.

Parrot, M., J. A. Sauvaud, J. J. Berthelier, and J. P. Lebreton (2007), First in-situ observations of strong ionospheric perturbations generated by a powerful VLF ground-based transmitter, *Geophys. Res. Lett.*, *34*, L11,111, doi10.1029/2007GL029368.

Piddyachiy, D., U. S. Inan, T. F. Bell, N. G. Lehtinen, and M. Parrot (2008), DEMETER observations of an intense upgoing column of ELF/VLF radiation excited by the HAARP HF heater, *J. Geophys. Res.*, *113*, A10308, doi10.1029/2008JA013208.

Ratcliffe, J. A. (1959), *The Magneto-Ionic Theory and Its Applications to the Ionosphere*, Cambridge University Press, Cambridge, U.K.

Rodriguez, J. V., and U. S. Inan (1994), Electron density changes in the nighttime D region due to heating by very-low-frequency transmitters, *Geophys. Res. Lett.*, *21*(2), 93–96.

Shao, X., B. Eliasson, A. S. Sharma, G. Milikh, and K. Papadopoulos (2012), Attenuation of whistler waves through conversion to lower hybrid waves in the low-altitude ionosphere, *J. Geophys. Res.*, *117*, A04311, doi10.1029/2011JA017339.

Singh, R., M. B. Cohen, A. K. Maurya, B. Veenadhari, S. Kumar, P. Pant, R. K. Said, and U. S. Inan (2012), Very low latitude (L = 1.08) whistlers, *Geophys. Res. Lett.*, *39*, L23102, doi10.1029/2012GL054122.

Spasojevic, M., and U. S. Inan (2005), Ground based VLF observations near L = 2.5 during the Halloween 2003 storm, *Geophys. Res. Lett.*, *32*, L21103, doi10.1029/2005GL024377.

Starks, M. J., R. A. Quinn, G. P. Ginet, J. M. Albert, G. S. Sales, B. W. Reinisch, and P. Song (2008), Illumination of the plasmasphere by terrestrial very low frequency transmitters: Model validation, *J. Geophys. Res.*, *113*, A09320, doi10.1029/2008JA013112.

Swamy, A. C. B. (1992), Equatorial electrojet parameters and the relevance of electromagnetic drifts (EMD) over Thumba, *Astrophys. Space Sci.*, *191*, 203–211.

Tao, X., J. Bortnik, and M. Friedrich (2010), Variance of transionospheric VLF wave power absorption, *J. Geophys. Res.*, *115*, A07303, doi10.1029/2009JA015115.

Wait, J. R. (1970), *Electromagnetic Waves in Stratified Media,* 2nd ed., Pergamon, New York.